First Performance Results of PTB's Atomic Caesium Fountain and a Study of Contributions to its Frequency Instability

Stefan Weyers, Andreas Bauch, Udo Hübner, Roland Schröder, and Christian Tamm

***Abstract*—At the Physikalisch-Technische Bundesanstalt (PTB), an atomic caesium fountain was constructed. Ramsey fringes with a full width at half maximum (FWHM) of 0.86 Hz were obtained by launching the atoms to a height of 83 cm above the cooling region (40 cm above the microwave cavity center). A first measurement of the homogeneity of the magnetic flux density yields 0.33 nT (rms), only 0.16% of the mean value of 0.205 μT used in normal operation. The inherent elementary noise contributions of the fountain and of a thermal beam atomic clock are compared in some detail.**

I. Introduction

The emergence of laser cooling techniques has stimulated the development of atomic caesium frequency standards based on cold atoms. Motivated by the outstanding results of the first caesium fountain frequency standard at the Laboratoire Primaire du Temps et des Fréquences (LPTF) in Paris [1], several groups worldwide have initiated programs to construct caesium fountains. With the LPTF fountain, the SI-second has been realized with the lowest uncertainty ($1.4 \cdot 10^{-15}$) ever obtained [2].

Also, at the PTB, an atomic caesium fountain was constructed to extend the time-keeping capabilities of the PTB's clock ensemble, consisting of several thermal beam atomic caesium clocks and three hydrogen masers. The fountain will be described subsequently, and some results will be reported.

One main advantage of an atomic fountain is its low frequency instability, eventually only limited by the quantum projection noise [3] [4]. As of yet, such a low noise level has not been reached with PTB's fountain. Hence, it is important to understand and characterize the individual noise contributions of the present system. This is the subject of Section IV, which also considers typical noise contributions of thermal atomic beam clocks for comparison. It is shown that, in the case of such clocks, the quantum projection noise can be considered to be included in the shot noise of the detected atoms. In a fountain, the effect of the shot-to-shot number variations of detected atoms is almost completely eliminated by proper normalization of the detected signal [1]. However, in the present PTB fountain set-up, we have to take into account that, because of the shot-to-shot fluctuations of the number of atoms in the respective sublevels (F, m_F), there is additional partition noise described by the binomial distribution law. With an adequately designed optical detection system, both photon shot noise and detection noise of the photodetector play a minor role; therefore, we are mainly concerned with the local oscillator noise [5], the partition noise, and the quantum projection noise.

In fact, the known dependence of the total noise on the number of detected atoms enables us to determine this number by a noise measurement, thus avoiding troublesome calculations based on the time-of-flight signal [4].

Manuscript received July 2, 1999; accepted October 26, 1999.

The authors are with Physikalisch-Technische Bundesanstalt, D-38116 Braunschweig, Germany (StefanWeyers@ptb.de).

II. The Fountain Set-up

In our fountain, about 10^7 caesium atoms are collected in a magneto-optical trap (MOT), cooled to less than 2.5 μK in optical molasses, pumped to the ground state level $F = 4$, and launched to a height of 83 cm. On their ballistic flight, the atoms pass two times through a TE011 microwave cavity [6] located about 43 cm above the MOT, where $(F = 4, m_F) \rightarrow (F = 3, m_F)$ ground state transitions are induced by the microwave field. The population of the ground state hyperfine levels is probed by fluorescence detection in a region 10 cm above the MOT.

Detection is performed using a similar scheme as in the LPTF fountain [1]. When the atoms cross a first transverse standing-wave light field tuned to the $F = 4 \rightarrow F' = 5$ transition, the fluorescence signal detected by a photodiode yields the number of atoms N_4 in the state $F = 4$. These atoms are then pushed away by a transverse traveling laser wave tuned to the same transition. The atoms in the state $F = 3$ are detected in a lower-lying zone by a second standing-wave field, which consists of a superposition of light tuned to the $F = 3 \rightarrow F' = 4$ and the $F = 4 \rightarrow F' = 5$ transitions. In this field, the atoms are first pumped to the state $F = 4$ and then are detected by their fluorescence in the same manner as the atoms in the upper detection channel to determine the number of atoms N_3 in the state $F = 3$. The fraction $N_{34} = N_3/(N_3 + N_4)$ indicates the transition probability associated with the microwave excitation. If we plot N_{34} against the frequency ν of the microwave field, we obtain Ramsey fringes as shown in Fig. 2, where the FWHM of the central peak is 0.86 Hz.

The laser diode system used for cooling and detecting the atoms consists of two extended cavity diode lasers (100 mW) locked to the $F = 4 \rightarrow F' = 5$ and $F = 3 \rightarrow$

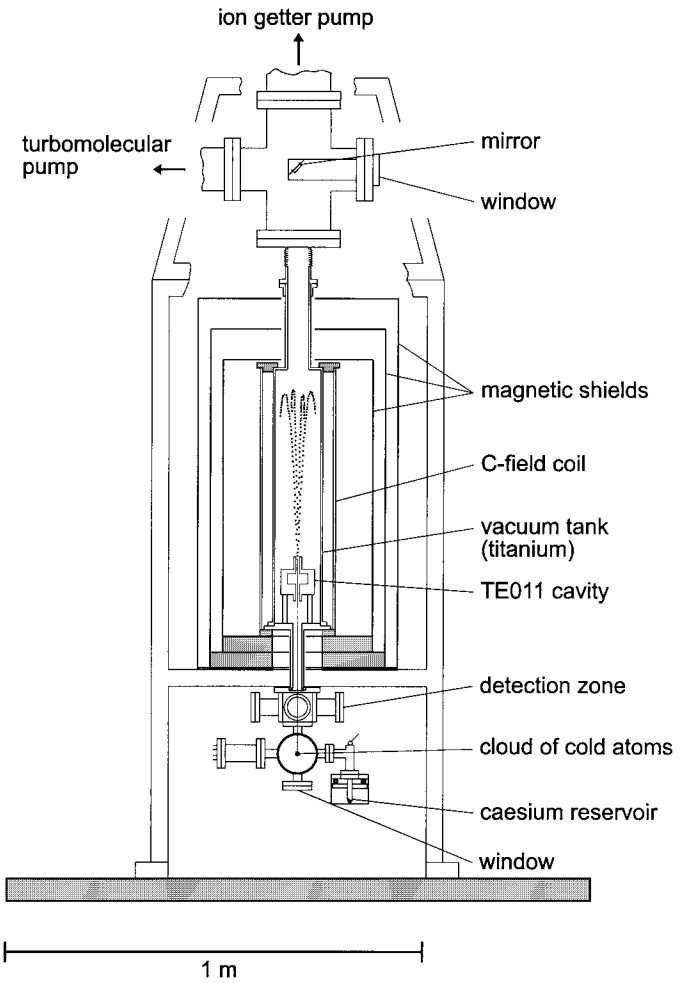

Fig. 1. Sketch of the atomic caesium fountain at PTB.

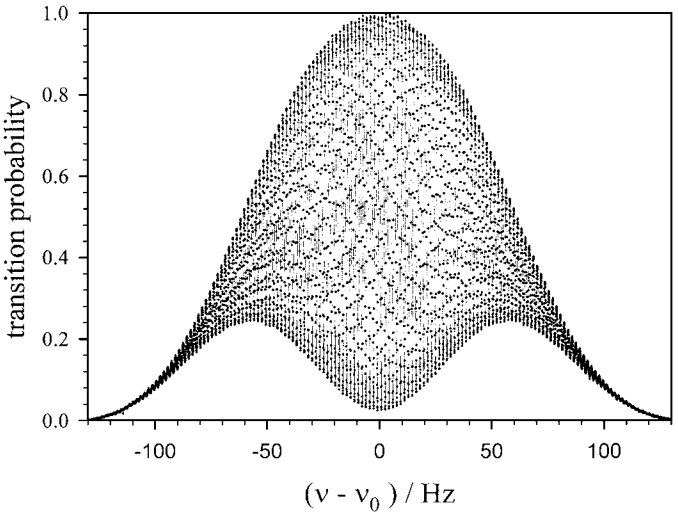

Fig. 2. Ramsey fringes of the microwave clock transition $(4,0) \rightarrow (3,0)$. Each point corresponds to one cycle of loading the trap and launching and detecting the atoms for a given microwave frequency detuning from $\nu_0 = 9\ 192\ 631\ 770$ Hz. The atoms were launched to 40 cm above the microwave cavity center. Lines between data points are only for guiding the eye.

$F' = 4$ transitions, respectively. The first laser is used as a master oscillator to injection lock a 200-mW laser diode, which provides the six cooling laser beams. The main part of the master laser light is used to detect the atoms. The other extended cavity diode laser serves as a repumping laser. The frequencies and intensities of the laser beams are controlled by acousto-optical modulators, which are also used in combination with mechanical shutters to switch off the laser beams in the time between launching and detection. The laser light is guided from the optical table to the fountain by polarization-maintaining optical fibers [6].

The microwave interrogation field of the fountain is synthesized from a low-noise 5-MHz quartz oscillator (Oscilloquartz OCXO 8611/02, Oscilloquartz, Neuchâtel, Switzerland), which is phase locked to the quartz oscillator of the PTB hydrogen maser H2 (KVARZ CH1-75, KVARZ, Nizhny Novgorod, Russia). The oscillator signal is multiplied to 9.2 GHz and mixed with the signal of a DRO (dielectric resonator oscillator). The beat signal is mixed with the signal of a frequency synthesizer locked to the 5-MHz low-noise quartz oscillator. The output of the mixer is used to phase lock the DRO, whose output frequency is the interrogation frequency for the fountain.

III. Magnetic Field Homogeneity

The most important frequency correction in caesium frequency standards is the frequency shift caused by the static magnetic field (C-field), which removes the degeneracy of the magnetic substates. In the PTB fountain, a static magnetic field of 0.205 μT is produced by a long coil surrounding the titanium vacuum chamber. At the top and at the bottom of the vacuum chamber, several compensation coils extend the area of high magnetic field homogeneity and provide adiabatic atomic transport from the cooling region to the C-field region, thus avoiding Majorana transitions [7]. The clock transition $(4,0) \rightarrow (3,0)$ has a small frequency shift proportional to $< B^2 >$, which is the mean squared magnetic flux density averaged over the flight path above the microwave cavity. The shift is given by

$$\Delta\nu_B = 427.45 \cdot 10^8 \frac{Hz}{T^2} \cdot < B^2 > . \qquad (1)$$

At $< B^2 >= (0.2\ \mu T)^2$, this shift is 1.7 mHz or $1.9 \cdot 10^{-13}$ in relative units. For correction of this shift, it is important to measure the magnetic flux density along the atomic flight path. An atomic fountain provides the possibility of mapping the C-field by launching the atoms to different heights and measuring the frequency shift of a field-sensitive transition (e.g., the $(4,-1) \rightarrow (3,-1)$ transition) for each height [1]. From this measurement, the magnetic field strength above the cavity $B(h)$ can be calculated. After a first homogenization of the magnetic field by adjustment of the compensation coil currents, a field map as shown in Fig. 3 was obtained.

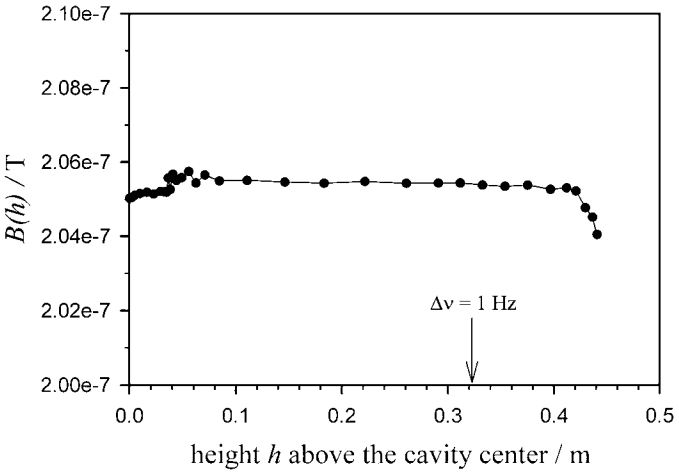

Fig. 3. Variation of the axial magnetic field strength along the axis of the PTB fountain above the microwave cavity. The arrow indicates the launching height to obtain a 1 Hz (FWHM) fringe width.

With increasing launching height, the number of Ramsey fringes increases, and it becomes difficult to identify the central Ramsey fringe. This is all the more true if the magnetic field is inhomogeneous at the apogee close to the upper end of the magnetic shieldings. In this case, the extension of the atomic cloud results in different mean magnetic field values for different parts of the cloud, which, in turn, gives different shifts of the related resonance signal contributions. Because of the constructive or destructive interference between these contributions, the resonance signal may show distinct side maximums, which can be misinterpreted as the position of the central fringe. To avoid misinterpretations, we started launching the atoms just up to the cavity, obtaining unambiguously the (only) central fringe, and continued by increasing steadily the launching height while observing the position of the three central fringes.

If the value $< B >^2$ obtained from the shift of the central fringe of the $(4,-1) \rightarrow (3,-1)$ transition is used for calculating $\Delta\nu_B$ according to (1), $\Delta\nu_B$ is miscalculated by the amount [8]

$$\delta\left[\Delta\nu_B\right] = 427.45 \cdot 10^8 \frac{Hz}{T^2} \cdot \sigma_B^2 \tag{2}$$

where σ_B is the inhomogeneity of the magnetic field. From the data points of Fig. 3, we obtain $\sigma_B = 0.33$ nT, so that $\delta[\Delta v_B]$ is $5 \cdot 10^{-19}$ (in relative units), which is negligible.

First comparisons of changes of the magnetic field inside the magnetic shieldings with changes of the ambient magnetic field yielded a satisfactory axial magnetic shielding factor of 4000.

IV. Noise Contributions and Frequency Instability

Recently, it has been shown [4] that, in an atomic fountain frequency standard, the noise limit given by the quantum projection noise [3] can be reached. For this purpose, all other relevant noise sources, such as photon shot noise and technical noise of the detection system, have to be carefully reduced. Because of the extremely high demands concerning local oscillator noise [5], the outstanding stability of a cryogenic sapphire resonator [9] appears to be indispensable.

To get more insight into the noise processes involved in our caesium fountain, we first consider the noise in a simple model of a thermal beam atomic clock. Because in practical devices the clock signal is given by the number of atoms in only one of the hyperfine states and not by $N_{34} = N_3/(N_3 + N_4)$ as in our fountain, the noise limit is given by the shot noise of the atomic beam hitting the Langmuir-Taylor detector. In our model, the atoms enter the first microwave interaction zone of the Ramsey cavity in the state $F = 4$, and the microwave frequency is tuned to obtain, on average, one-half of the atoms with $m_F = 0$ in the state (4,0) and one-half of the atoms in the state (3,0) behind the cavity. In this case, the transition probability associated with the microwave excitation is $p = 1/2$. Only the number $N_{(3,0)}$ of atoms in the state (3,0) is detected. One way of describing this measurement process is to state that the Poisson distribution law, which describes the shot noise of the atom detection, gives, for the measured mean value $\bar{N}_{3,O}$, an uncertainty $\sigma_{(3,0)} = \sqrt{\bar{N}_{(3,0)}}$. If the mean number of atoms leaving the Cs oven is given by $\bar{N}^O$ and we assume that the number of atoms in the state (4,0) is 1/16 of $\bar{N}^O$ and that no atoms are lost during the flight path, we obtain

$$\bar{N}_{(3,0)} = 1/16 \cdot p \cdot \bar{N}^O = 1/16 \cdot 1/2 \cdot \bar{N}^O \tag{3}$$

so that

$$\sigma_{(3,0)} = \sqrt{\bar{N}_{(3,0)}} = \sqrt{\bar{N}^O/32.} \tag{4}$$

Eq. (3) and (4) do not explicitly indicate the quantum projection noise contribution. To recognize this contribution, we chose an alternative description of the measurement process, which is shown in the following paragraphs.

Because of the Poisson distribution law, the noise of the atomic beam leaving the oven is $\sigma^O = \sqrt{\bar{N}^O}$. The noise of the part of the atomic beam containing only the atoms in the state (4,0) is given by

$$\sigma_{(4,0)} = \sqrt{\bar{N}^O/16.} \tag{5}$$

This equation can also be deduced from the following considerations. A noise contribution $\sigma'_{(4,0)} = \sqrt{\bar{N}^0}/16$ would result in the case of vanishing sublevel population partition noise. The partition noise contribution is given by the binomial distribution law and amounts to $\sigma_{bi} = \sqrt{\bar{N}^O} \cdot \sqrt{p' \cdot (1-p')}$ with $p' = 1/16$. Assuming statistically independent noise contributions, the total noise is

$$\sigma_{(4,0)} = \sqrt{\left(\sigma'_{(4,0)}\right)^2 + (\sigma_{bi})^2} = \sqrt{\bar{N}^O/16,} \tag{6}$$

which is in fact the same result as obtained previously (5).

Now, we proceed in a similar manner when taking into account the microwave interaction. If exactly one-half of the atoms in the state (4,0) would be transferred to the state (3,0), the corresponding detection noise would be given by

$$\sigma^d_{(3,0)} = 1/2 \cdot \sigma_{(4,0)} = 1/2 \cdot \sqrt{\bar{N}^O/16}. \tag{7}$$

Actually, only an average of one-half of the atoms that enter the microwave cavity is detected in the state (3,0) after excitation. This is due to the quantum projection noise, which is also determined by the binomial distribution law [3]. In our case ($p = 1/2$), the quantum projection noise contribution amounts to

$$\sigma_{qp} = \sqrt{\bar{N}^O/16} \cdot \sqrt{p \cdot (1-p)} = \sqrt{\bar{N}^O/16} \cdot 1/2. \tag{8}$$

Because the noise contributions (7) and (8) are statistically independent, the total noise is given by

$$\sigma = \sqrt{\left(\sigma^d_{(3,0)}\right)^2 + (\sigma_{qp})^2} = \sqrt{\bar{N}^O/32}. \tag{9}$$

Eq. (9) is identical to the result (4) that was obtained by considering the shot noise of the atoms that are actually detected. This demonstrates that, in a thermal beam atomic clock, the shot noise of the detected atoms already includes the quantum projection noise.

Now, we use similar arguments for the estimate of the noise of the fountain signal N_{34}. As mentioned previously, the shot-to-shot fluctuations of the total number of detected atoms are eliminated almost completely by the normalizing detection system. Because of optical pumping in the molasses, the atoms are distributed among the nine $(4, m_F)$ substates. In our fountain, after launching, and in the detection zone, we find an average of 1/8 of the total number of atoms with a quantum number of $m_F = 0$. Hence, we get a sublevel population partition noise contribution calculated from the binomial distribution law

$$\sigma^{FO}_{bi} = \frac{1}{2} \cdot \sqrt{N_{at}} \cdot \sqrt{1/8 \cdot (1-1/8)}/N_{at}. \tag{10}$$

$N_{at} = N_3 + N_4$ is the total number of the detected atoms. The factor one-half is again due to the fact that we assume that exactly one-half of the atoms in the state (4,0) are transferred to the state (3,0). Actually, there is again a quantum projection noise contribution, which is given by

$$\sigma^{FO}_{qp} = \sqrt{N_{at}/8} \cdot \sqrt{1/2 \cdot (1-1/2)}/N_{at} \tag{11}$$

where we take into account that only $N_{at}/8$ of the atoms undergo the microwave transition with $p = 1/2$. Assuming independent noise contributions, the total noise is then given by

$$\sigma^{FO} = \sqrt{\frac{7}{256}\frac{1}{N_{at}} + \frac{1}{32}\frac{1}{N_{at}} + \frac{15}{256}\frac{1}{N_{at} n_{ph}} + \frac{113}{128}\frac{\sigma^2_{det}}{N^2_{at}} + \sigma^2_{l.o.}} \tag{12}$$

where the first two terms indicate the sublevel partitition noise and the quantum projection noise, respectively. The third term is due to the photon shot noise. The fourth term is due to the photodetection background noise σ_{det}, and the last term represents a noise contribution $\sigma_{l.o.}$ caused by the local oscillator. The photon shot noise contribution can usually be neglected because n_{ph}, the number of detected photons per atom, can easily be made larger than 100.

The situation described by (12) can be compared with the case in which the same number of atoms is launched but atoms in the state $m_F = 0$ are selected immediately after the launching [1], [4]. Hence, there is no sublevel partition noise; the number of detected atoms in the states (3,0) and (4,0) is $N'_{at} \sim 1/8 N_{at}$, and the total noise becomes

$$\sigma^{FO}_{ps} = \sqrt{\frac{1}{4N'_{at}} + \frac{1}{4N'_{at} n_{ph}} + \frac{\sigma^2_{det}}{2N'^2_{at}} + \sigma^2_{l.o.}}. \tag{13}$$

Because the noise of (12) corresponds to a signal $N_{34} = 1/2 \cdot 1/8 = 1/16$, and the noise of (13) corresponds to a signal of $N_{34} = 1/2 \cdot 1 = 1/2$, it can be seen that, for the same number of launched atoms, the signal-to-noise ratio is only increased by a factor of about 1.37, if $m_F = 0$ preselection is applied and if the photon shot noise, detection noise, and local oscillator noise are negligible.

If we operate the fountain in resonance ($\nu = \nu_0 =$ 9 192 631 770 Hz) at one-half the optimum microwave power, the atoms experience, during their two consecutive passes through the microwave cavity, two $\pi/4$ pulses ($p = 1/2$). Thus, again we obtain one-half of the atoms with $m_F = 0$ in the state (4,0) and the other half in the state (3,0), but without being sensitive to the local oscillator noise, so that, neglecting the photon shot noise, (12) becomes

$$\sigma^{FO} = \sqrt{\frac{15}{256}\frac{1}{N_{at}} + \frac{113}{128}\frac{\sigma^2_{det}}{N^2_{at}}}. \tag{14}$$

With a signal of $N_{34} = 1/16$, the signal-to-noise ratio becomes

$$\frac{N_{34}}{\sigma^{FO}} = \frac{1}{\sqrt{15\frac{1}{N_{at}} + 226\frac{\sigma^2_{det}}{N^2_{at}}}}. \tag{15}$$

We measured this ratio for different numbers of launched atoms by varying the loading time of the MOT and detecting the variance of N_{34}. Recording the size of the area below the time-of-flight signal ($F = 4$) yields a signal N_{TOF}, which is proportional to the total number of detected atoms N_{at}. A least squares fit of the experimental values with $r = N_{at}/N_{TOF}$ and σ_{det} as free parameters yields $\sigma_{det} \approx 87(15)$ atoms and $r = 57\ 500(8800)$ atoms, so that we can calculate N_{at} from the measured signal-to-noise ratio (15) with an uncertainty of 15% similarly as in [4]. The experimental values are shown in Fig. 4 together with the fit. The indicated number of atoms N_{at} was calculated from the fit results. At low atom numbers,

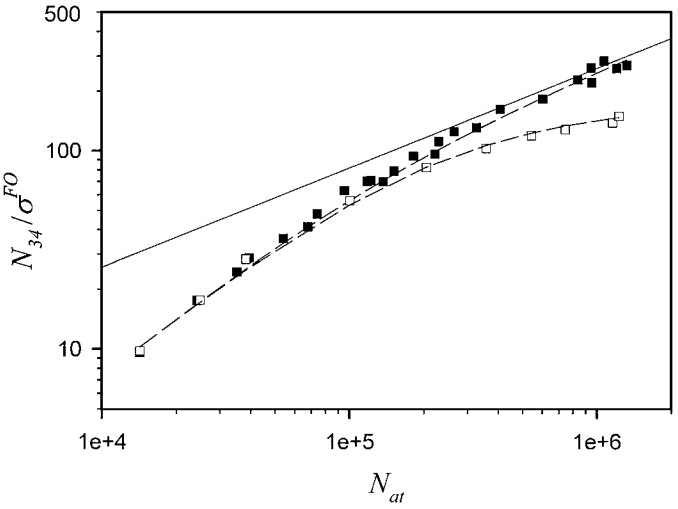

Fig. 4. Signal-to-noise ratio as it depends on the number of detected atoms. The black squares are data points obtained by operating the fountain with two $\pi/4$ pulses. The open squares are data points obtained by operating at $\nu = \nu_0 + \mathrm{FWHM}/2$ at optimum microwave power. The dashed lines are fit to the data points, and the full line indicates the signal-to-noise ratio, if only partition and quantum projection noise contribute to the total noise.

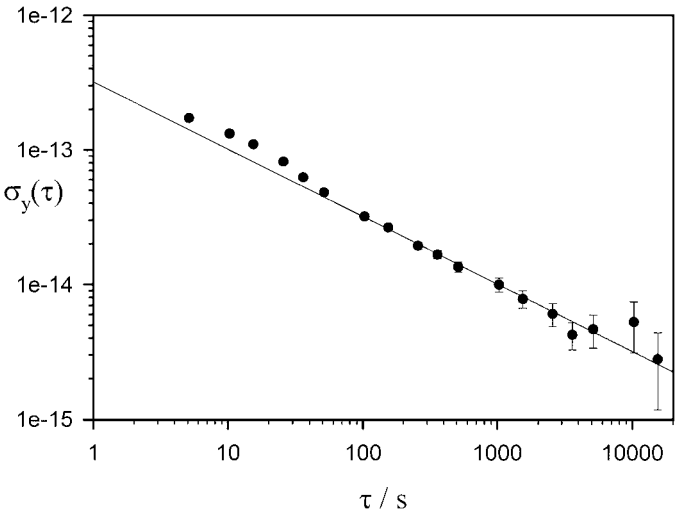

Fig. 5. Relative frequency instability $\sigma_y(\tau)$ of measured frequency differences between the PTB fountain and hydrogen maser H2. The line is a least squares fit to the data ($\tau \geq 100$ s) assuming $\sigma_y(\tau)$ to be proportional to $\tau^{-1/2}$.

the signal-to-noise ratio is proportional to N_{at} and limited by the detection noise. For high atom numbers, the slope changes and the signal-to-noise ratio becomes proportional to $(N_{at})^{1/2}$ because, in this case, the noise is dominated by the partition and the quantum projection noise.

When the fountain is operated at $\nu = \nu_0 + \mathrm{FWHM}/2$ at optimum microwave power (again $p = 1/2$), the influence of the local oscillator noise on the signal-to-noise ratio becomes visible, as shown in Fig. 4. The signal-to noise ratio is given by

$$\frac{N_{34}}{\sigma^{FO}} = \frac{1}{\sqrt{15\frac{1}{N_{at}} + 226\frac{\sigma^2_{det}}{N^2_{at}} + 256\sigma^2_{l.o.}}}. \qquad (16)$$

For low atom numbers, this ratio is again proportional to N_{at} and coincides with the signal-to-noise ratio obtained in the first case because the main noise contribution is due to the detection noise. For high atom numbers, the signal-to-noise ratio saturates because of the local oscillator noise $\sigma_{l.o.}$.

Comparing the signal-to-noise ratio for both cases, we find that, for $1.2 \cdot 10^6$ detected atoms, the signal-to-noise ratio decreases from 270 to 146 because of the local oscillator noise. If we perform a least squares fit for the latter case by adding another free parameter to take into account the noise contribution caused by the local oscillator, we obtain, for the Allan standard deviation of the quartz oscillator currently in use, $\sigma_y(1s) \approx 1.7(4) \cdot 10^{-13}$.

We limited our measurements to the regime up to about 10^6 detected atoms. In this regime, about 10^5 atoms contribute to the clock signal of the $(4,0) \rightarrow (3,0)$ transition. Because of the instability of the employed quartz oscillators, larger atom numbers would not have increased the signal-to-noise ratio. We measured relative frequency differences between the PTB fountain and the hydrogen maser H2. The modulation width of the computer-controlled synthesizer and thus of the DRO was equal to the FWHM $\Delta\nu = 0.86$ Hz of the central Ramsey fringe. By recording the slope at FWHM of the central Ramsey fringe and N_{34} on both sides of the fringe, the frequency difference between the fountain and H2 is calculated. Operating the fountain at 10^6 detected atoms per cycle (cycle time $T_C = 2.56$ s) resulted in a relative frequency instability of $\sigma_y(\tau) = 3.2(1) \cdot 10^{-13}\tau^{-1/2}$ (100 s $\leq \tau \leq$ 15 000 s). A plot of $\sigma_y(\tau)$ is shown in Fig. 5. The slight increase of $\sigma_y(\tau)$ for smaller values of τ is probably due to the servo-lock of the quartz oscillator to the hydrogen maser. Finally, $\sigma_y(\tau)$ is in agreement with the measured signal-to-noise ratio (142 at 10^6 detected atoms) of the fountain signal according to

$$\sigma_y = \frac{1}{\pi Q_{at}} \frac{\sigma^{FO}}{N_{34}} \sqrt{\frac{T_C}{\tau}} \qquad (17)$$

with the atomic quality factor $Q_{at} = \nu_0/\Delta\nu$.

V. Conclusion

We have reported on first measurements on an atomic caesium fountain recently assembled at PTB. First Ramsey fringes were obtained with a fringe width well below 1 Hz. Investigations of magnetic field homogeneity and stability showed good results. In the near future, we will proceed toward a comprehensive uncertainty evaluation of the fountain.

Furthermore, it is planned to install a second microwave cavity, which will allow the selection of atoms in a single substate (3,0) for the ballistic flight [1]. Then, it is expected that, for the same number of launched atoms, the instability will be improved by a factor of 1.37. At the

same time, the collisional shift will be reduced by a factor of 4.5 because the density is reduced by a factor of 9 and the collisional shift caused by atoms preselected in the state (3,0) is twice the shift caused by atoms distributed among all the states $(4, m_F)$ [10].

References

[1] A. Clairon, S. Ghezali, G. Santarelli, Ph. Laurent, S. N. Lea, M. Bahoura, E. Simon, S. Weyers, and K. Szymaniec, "Preliminary accuracy evaluation of a cesium fountain frequency standard," in *Proc. 5th Symp. Freq. Standards and Metrology*, Woods Hole, MA, Singapore: World Scientific Publishing, 1997, pp. 49–59.

[2] Consultative Committee on Time and Frequency, 14th session, *Working Doc. CCTF99-11*, 1999.

[3] W. M. Itano, J. C. Bergquist, J. J. Bollinger, J. M. Gilligan, D. J. Heinzen, F. L. Moore, M. G. Raizen, and D. J. Wineland, "Quantum projection noise: Population fluctuations in two-level systems," *Phys. Rev. A*, vol. 47, pp. 3554–3570, May 1993.

[4] G. Santarelli, Ph. Laurent, P. Lemonde, A. Clairon, A. G. Mann, S. Chang, A. N. Luiten, and C. Salomon, "Quantum projection noise in an atomic fountain: A high stability cesium frequency standard," *Phys. Rev. Lett.*, vol. 82, pp. 4619–4622, Jun. 1999.

[5] G. J. Dick, "Local oscillator induced instabilities in trapped ion frequency standards," in *Proc. Precise Time and Time Interval Mtg.*, Redondo Beach, CA, pp. 133–147, 1987.

[6] U. Hübner, S. Weyers, J. Castellanos, D. Griebsch, R. Schröder, C. Tamm, and A. Bauch, "Progress of the PTB caesium fountain frequency standard," in *Proc. 12th Eur. Freq. Time Forum (EFTF)*, Warsaw, Poland, pp. 544–547, 1998.

[7] A. Bauch and R. Schröder, "Frequency shifts in a cesium atomic clock due to Majorana transitions," *Annalen der Physik*, vol. 2, no. 5, pp. 421–449, 1993.

[8] S. Weyers, A. Bauch, D. Griebsch, U. Hübner, R. Schröder, and C. Tamm, "First results of PTB's atomic caesium fountain," in *Proc. Joint Mtg. Eur. Freq. Time Forum and IEEE Int. Freq. Contr. Symp.*, Besançon, France, pp. 16–19, 1999.

[9] A. N. Luiten, A. G. Mann, M. E. Costa, and D. G. Blair, "Power stabilized cryogenic sapphire oscillator," *IEEE Trans. Instr. Meas.*, vol. 44, pp. 132–135, Apr. 1995.

[10] S. Ghezali, Ph. Laurent, S. N. Lea, and A. Clairon, "An experimental study of the spin-exchange frequency shift in a laser-cooled cesium fountain frequency standard," *Europhys. Lett.*,, vol. 36, pp. 25–30, Oct. 1996.

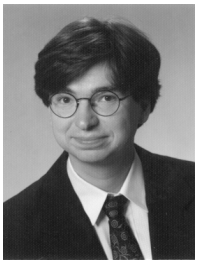

Stefan Weyers was born in Wuppertal, Germany, in 1962. He received the Dipl.-Phys. and Dr.rer.nat. degrees in physics from the Westfälische-Wilhelms Universität, Münster, Germany, in 1988 and 1994, respectively.

From 1990 to 1991, he worked on grazing ion-surface collisions at the Institut für Kernphysik, Universität Münster. In 1996, he joined the Laboratory for Time and Frequency, Physikalisch-Technische Bundesanstalt (PTB), Braunschweig, Germany, while a Ph.D.-student. From 1995 to 1996, he was a postdoc at the French Laboratoire du Temps et des Fréquences (LPTF), Paris, and the French Laboratoire de l'Horloge Atomique (LHA), Orsay, where he was engaged in research on cold atoms and frequency standards. In 1996, he joined again PTB, where he is currently engaged in research on atomic fountains.

Andreas Bauch was born in Wiesbaden, Germany, in 1957. He received the Dipl.-Phys. and Dr.rer.nat. degrees in physics from Johannes Gutenberg University, Mainz, Germany, in 1982 and 1986, respectively.

In 1983, he joined the Laboratory for Time and Frequency, Physikalisch-Technische Bundesanstalt (PTB), Braunschweig, Germany, while a Ph.D.-student. In 1988, he started research work on frequency standards based on trapped Yb ions. Since 1990, he has been head of PTB's time unit section.

Udo Hübner was born in Groß-Wierau, Silesia, Germany, on October 26, 1937. He received the Dipl.-Phys. and Dr.rer.nat. degrees from the Technische Universität of Braunschweig, Braunschweig, Germany, in 1966 and 1972, respectively.

From 1964 to 1972, he worked at the Technische Universität of Braunschweig on problems in solid-state theory, especially on conductivity and crystal fault problems. Since 1972, he has been with the Physikalisch-Technische Bundesanstalt (PTB), Braunschweig, Germany, where his research was in the fields of statistical aspects of time scales, laser dynamics (chaos), and interaction of laser light and atoms. Presently he is engaged in research on atomic fountains.

Roland Schröder was born in Helmstedt, Germany, in 1943. He received the Dipl.-Ing. degree in electrical engineering in 1970 from the Technische Universität, Braunschweig, Germany.

From 1970 to 1971, he was engaged with the development of navigation systems at Anschütz, Kiel, Germany. He joined the Physikalisch-Technische Bundesanstalt, Braunschweig, in 1972, where he is now responsible for the development of the electronics and microwave components of primary clocks.